

Pentaquark P_c electroproduction in $J/\psi + p$ channel in electron-proton collisions

Ya-Ping Xie,^{1,2,*} Xu Cao,^{1,2,†} Yu-Tie Liang,^{1,2,‡} and Xurong Chen^{1,2,3,§}

¹*Institute of Modern Physics, Chinese Academy of Sciences, Lanzhou 730000, China*

²*University of Chinese Academy of Sciences, Beijing 100049, China*

³*Institute of Quantum Matter, South China Normal University, Guangzhou 510006, China*

Abstract

Pentaquark states electro- and photo-production is an unique platform to disentangle their nature due to the potential absence of triangle singularity. To this end, the eSTARlight package is adapted to study the electroproduction of pentaquark P_c states, discovered first by LHCb, in the $ep \rightarrow eJ/\psi p$ process at electron-ion colliders (EICs). The results are compared to the non-resonant t -channel, which is described by the Pomeron exchange in our studies. We address the difference of proposed EICs in China and USA from intermediate to high energy configuration and explore their potential of searching for pentaquark P_c states with the help of J/ψ production in electron-proton scattering.

PACS numbers: 24.85.+p, 12.38.Bx, 12.39.St, 13.88.+e

arXiv:2003.11729v2 [hep-ph] 27 Mar 2020

* xieyaping@impcas.ac.cn

† caoxu@impcas.ac.cn

‡ liangyt@impcas.ac.cn

§ xchen@impcas.ac.cn

I. INTRODUCTION

Up to now a rich spectrum of the exotic mesons, including charmonium-like and bottomonium-like states, is emerging, and more new states are expected for the continuing experimental effort [1–8]. However, in the baryon sector only three narrow pentaquark states, $P_c(4312)$, $P_c(4440)$ and $P_c(4457)$, are discovered by the LHCb collaboration in $\Lambda_b \rightarrow J/\psi p K^-$ decay [9, 10]. It is essential to study these known states and search for new states by other decay and reaction channels in order to disentangle different models. Just recently, D0 and GlueX collaborations have searched for these states in inclusive $p\bar{p}$ collisions [11] and photoproduction [12], respectively. The D0 collaboration found an enhancement from joint contribution of $P_c(4440)$ and $P_c(4457)$ in $J/\psi p$ invariance mass spectrum with low significance [11], serving as the first and only confirmatory evidence for these pentaquark states. Various interpretations were proposed for the nature of hidden charm pentaquark states before and after their observation, e.g. molecular states [13, 14], compact diquark-diquark-antiquark states [15–17], and hadro-charmonium states [18]. In addition, it is pointed out that the peaks of pentaquark in the decay and reactions with multi-particle final states could be induced by triangle singularity considering that their masses locate close to the $\Sigma_c \bar{D}$ and $\Sigma_c \bar{D}^*$ threshold [19–25]. In order to survey this non-resonance explanation, the reactions with two-body final states induced by beams of photon, electron [26–32] and pion [21, 33–35] are suggested to be decisive. At present and in the near future, the high energy pion beam seems to be unavailable, so photo- and electroproduction reactions would play the central role and attract much interest. These reactions are also useful to search for other P_c , for instance those among seven states in spin multiplets anticipated by heavy-quark spin symmetry [36–38], and also P_b , the bottom analogs of P_c , expected by heavy quark flavor symmetry in many models [27, 39–42].

Though GlueX group did not find the photoproduction of pentaquark states with present precision [12], a very meaningful upper limit of production cross sections, and hence a model dependent upper limit of branching ratios $\mathcal{B}(P_c \rightarrow J/\psi p)$, are given by their data. Combining the measured decay ratios from LHCb with a simple expectation of $\mathcal{B}(\Lambda_b \rightarrow P_c^+ K^-)$, a reasonable estimation of the lower limit of $\mathcal{B}(P_c \rightarrow J/\psi p)$ could be obtained [43]. So a stringent and confined range of the photoproduction cross section of pentaquark would be calculated, and the sole model uncertainty is from the assumed vector meson dominance (VMD). The non-resonant t -channel contribution is usually imitated by Pomeron or gluon exchange in these calculations, while the s -channel is mainly driven by the Breit-Wigner resonances.

In line with these ideas, we investigate the electroproduction of pentaquark P_c in $ep \rightarrow eJ/\psi p$ reaction with a great detail in this paper. In electron-proton scattering, the initial electron emits virtual photon which interacts with the initial proton to produce final particles. This process can be simulated by eSTARlight package[44, 45], which includes only t -channel for the beginning and is adapted to incorporate the s -channel here. As the basic ingredient, the $\gamma p \rightarrow J/\psi p$ is an important input for the electroproduction, which can be realized experimentally at JLab (and its update JLab12), and also electron-ion collider (EIC). There are several proposed EICs, for instance, EicC (EIC in China) [46, 47], eRHIC (EIC in US) [48] and LHeC (EIC in LHC) [49], ranging from intermediate to extremely high energies. Here we will concentrate on EicC and eRHIC by comparison of cross sections and the rapidity distributions of final particles.

This paper is organized as follows. The theoretical framework is given in Sec II. The

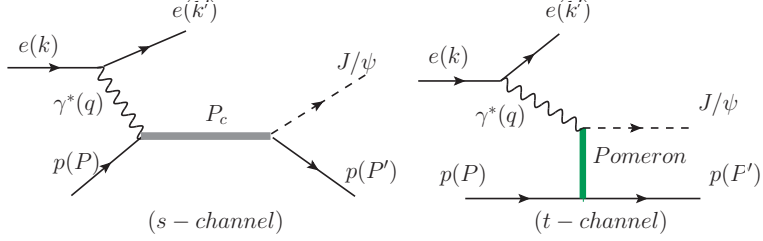


FIG. 1. (Color online) Feynman diagrams for J/ψ production in electron-proton scattering through P_c resonances s -channel (left graph) and Pomeron exchange t -channel (right graph).

numerical results are shown in Sec. III, closed with a summary in Sec. IV.

II. THEORETICAL FRAMEWORK

The diagrams for s -channel and t -channel processes of $ep \rightarrow eJ/\psi p$ are shown in Fig. 1. In s -channel, the virtual photon and initial proton produce resonances (e.g. P_c states here), and then the resonant states decay into $J/\psi p$. In t -channel, virtual photon interacts through Pomeron or gluon from proton and then convert into final J/ψ meson. In this paper we use the Pomeron exchange for t -channel. We parameterize these contribution for $\gamma p \rightarrow J/\psi p$, as the basic input to the simulation of $ep \rightarrow eJ/\psi p$ reaction. This can be recognized by the eSTARlight package, which is a Monte-Carlo simulation program for the vector meson production in electron-proton collisions [44, 45]. It can be also employed to study the various vector mesons production in electron-ion collisions.

In the electron-proton scattering, the cross section of the $ep \rightarrow eJ/\psi p$ in terms of the cross sections of the $\gamma^* p \rightarrow J/\psi p$ is given by [44],

$$\sigma(ep \rightarrow eJ/\psi p) = \int dk dQ^2 \frac{dN^2(k, Q^2)}{dk dQ^2} \sigma_{\gamma^* p \rightarrow J/\psi p}(W, Q^2). \quad (1)$$

where k is the momentum of the photon emitted from electron in target rest frame, W is the center of mass (c.m.) energy of the photon and proton system, and Q^2 is the virtuality of the photon. The photon flux reads as [50]

$$\frac{d^2 N(k, Q^2)}{dk dQ^2} = \frac{\alpha}{\pi k Q^2} \left[1 - \frac{k}{E_e} + \frac{k^2}{2E_e^2} - \left(1 - \frac{k}{E_e} \right) \left| \frac{Q_{min}^2}{Q^2} \right| \right]. \quad (2)$$

where E_e is the energy of the electron in target rest frame, and Q_{min}^2 is defined as

$$Q_{min}^2 = \frac{m_e^2 k^2}{E_e(E_e - k)}. \quad (3)$$

The maximum Q^2 is determined by the energy loss of the electron

$$Q_{max}^2 = 4E_e(E_e - k). \quad (4)$$

The Q^2 dependence of $\sigma_{\gamma^* p \rightarrow J/\psi p}(W, Q^2)$ is factorized as

$$\sigma_{\gamma^* p \rightarrow J/\psi p}(W, Q^2) = \sigma_{\gamma p \rightarrow J/\psi p}(W, Q^2 = 0) \left(\frac{M_V^2}{M_V^2 + Q^2} \right)^\eta. \quad (5)$$

where $\eta = c_1 + c_2(M_V^2 + Q^2)$ with the values of $c_1 = 2.36 \pm 0.20$ and $c_2 = 0.0029 \pm 0.43 \text{ GeV}^2$, which are determined by the data of $\gamma^*p \rightarrow J/\psi p$ with $Q^2 \neq 0$ [44]. We use the same Q^2 dependence for P_c and Pomeron channels, because of these values are unknown for P_c resonance channel. Because of the very strong Q^2 dependence of photon flux in Eq. (2), the impact of this prescription is expected to be not big for the final results.

For the P_c resonant channel, the cross section of $\gamma p \rightarrow J/\psi p$ can be written in a compact Breit-Wigner form[27, 28]

$$\sigma_{\gamma p \rightarrow J/\psi p}^{P_c}(W) = \frac{2J+1}{2(2s_2+1)} \frac{4\pi}{k_{in}^2} \frac{\Gamma_{P_c}^2}{4} \frac{\mathcal{B}(P_c \rightarrow \gamma p)\mathcal{B}(P_c \rightarrow J/\psi p)}{(W - M_{P_c})^2 + \Gamma_{P_c}^2/4}. \quad (6)$$

with s_1 being the spin of initial proton and J is the total spin of P_c pentaquark. Here M_{P_c} and Γ_{p_c} is the mass and total decay width of the P_c states, respectively. The k_{in} is the magnitude of three momentum of initial state in the c.m. frame. The branching ratio of $P_c \rightarrow \gamma p$ is calculated by the vector meson dominant model:

$$\mathcal{B}(P_c \rightarrow \gamma p) = \frac{3\Gamma(J/\psi \rightarrow e^+e^-)}{\alpha M_{J/\psi}} \left(\frac{k_{in}}{k_{out}}\right)^{2L+1} \mathcal{B}(P_c \rightarrow J/\psi p). \quad (7)$$

with α being the fine structure constants and $\Gamma(J/\psi \rightarrow e^+e^-)$ the dilepton decay width of J/ψ . The k_{out} is the magnitude of three momentum of final state in the c.m. frame. In this work, we use the lowest orbital excitation $L = 0$ for $J/\psi p$ system and $J = 1/2$. Other quantum numbers of P_c can be similarly calculated. We adopt $\mathcal{B}(P_c \rightarrow J/\psi p) = 5\%$ for all P_c states, which are in the same level of the upper limits from GlueX group [12]. A comparison of our $\sigma_{\gamma p \rightarrow J/\psi p}^{P_c}(W)$ to the GlueX data could be found in Ref. [43].

In order to study the rapidity distributions and transverse momentum distributions of J/ψ and proton in final states, we need angular distributions of the decay process $P_c \rightarrow J/\psi p$. We assume the angle distributions of $P_c \rightarrow J/\psi p$ in a following general expression

$$\frac{d\sigma}{d\cos\theta} \propto 1 + \beta \cos^2\theta. \quad (8)$$

Here θ is polar angle of J/ψ or proton in the rest frame of P_c states and β is dependent on the quantum number J^P of P_c pentaquark, if only lowest partial wave is considered. But usually several partial waves are presented in this work, so the actual value of β would deviate from these values. The relation of β and J^P are listed in Table.I. These results are employed in the calculation of the J/ψ rapidity dsistributions.

J^P	$\frac{1}{2}^-$	$\frac{1}{2}^+$	$\frac{3}{2}^-$	$\frac{3}{2}^+$
β	-1	0	0	1

TABLE I. β from different quantum number of P_c states.

For the contribution of t -channel Pomeron exchange, the cross section of $\gamma p \rightarrow J/\psi p$ is given as [51],

$$\sigma_{\gamma p \rightarrow J/\psi p}^t(W) = \sigma_p \cdot \left(1 - \frac{(m_p + m_{J/\psi})^2}{W^2}\right) \cdot W^\epsilon, \quad (9)$$

with $\sigma_p = 4.06 \text{ nb}$ and $\epsilon = 0.65$, which are determined by the experimental data of $\gamma p \rightarrow J/\psi p$ with $Q^2 = 0$ and applied successfully to previous studies of J/ψ electroproduction [51].

The interference between P_c resonance channel and Pomeron exchange channel is not considered at this paper just because it is too premature to include it. We employ eSTARlight to simulate P_c resonance production through photon proton interaction. Then, the decay process of $P_c \rightarrow J/\psi p$ is implemented in eSTARlight. Finally, the J/ψ to dilepton is simulated. The resonance channel production in eSTARlight is newly studied and it can be applied to considered other resonance channel in the next step.

III. NUMERICAL RESULT

The properties of $P_c(4312)$, $P_c(4440)$, and $P_c(4457)$ from LHCb are listed in Table II. Throughout this paper we use the central values of the masses and widths of three P_c states. We investigate their production in proposed EICs, including EicC and eRHIC, whose c.m. energies are also given in Table II. A detailed comparison of the proposed EICs are presented in Ref. [45, 46].

First of all, we list the estimated cross sections of $ep \rightarrow eP_c \rightarrow eJ/\psi p$ and range of the rapidity distribution of P_c states in Table II. For all the calculation in this work, we set $0 < Q^2 < 5\text{GeV}^2$. As can be seen, the electroproduction of P_c in $J/\psi p$ channel is a bit less than 1.0 pb. This indicates that these P_c states are measurable in these EICs with $\mathcal{B}(P_c \rightarrow J/\psi p) = 5\%$, even considering the dilepton decay ratios of J/ψ and the detector efficiency. If the $\mathcal{B}(P_c \rightarrow J/\psi p)$ is much less than 5%, then the open charm channels will have great potential for studying the P_c states, as pointed out by Ref. [42]. The production cross sections of $ep \rightarrow eP_c \rightarrow eJ/\psi p$ rise gently when the c.m energies of electron-proton are increasing, because most of the P_c is produced in small Q^2 range. The rapidity distribution of P_c is very limited, for the reason that P_c are narrow states produced in s -channel. From Table II, it can be seen that the P_c are produced closer to the mid-rapidity with lower c.m energies of electron-proton, e.g. at EicC than that at higher energies, namely eRHIC. Combining with these two aspects, it seems that very high c.m. energies of electron-proton is not required to study P_c states.

Resonance		Properties [10]	Collider	EicC	eRHIC
			\sqrt{s}	16.8 GeV	140.7 GeV
$P_c(4312)$	Mass	$4311.9 \pm 0.7^{+6.8}_{-0.6}$ GeV	Total cross section	0.35 pb	0.58 pb
	Decay width	$9.8 \pm 2.7^{+3.7}_{-4.5}$ MeV	Rapidity region	$-2.23 < y < -2.22$	$-4.86 < y < -4.84$
$P_c(4440)$	Mass	$4440.3 \pm 1.3^{+4.1}_{-4.7}$ GeV	Total cross section	0.53 pb	0.83 pb
	Decay width	$20.6 \pm 4.9^{+8.7}_{-10.1}$ MeV	Rapidity region	$-2.22 < y < -2.18$	$-4.84 < y < -4.80$
$P_c(4457)$	Mass	$4457.3 \pm 0.6^{+4.1}_{-1.7}$ GeV	Total cross section	0.16 pb	0.21 pb
	Decay width	$6.4 \pm 2.0^{+5.7}_{-1.9}$ MeV	Rapidity region	$-2.20 < y < -2.19$	$-4.82 < y < -4.81$

TABLE II. Total cross sections of $ep \rightarrow eP_c \rightarrow eJ/\psi p$ and rapidity region of three P_c states in proposed EicC and eRHIC. The positive direction of rapidity is along with the direction of electron.

Secondly, as we discuss in above section, the rapidity distributions of J/ψ are determined by the angle distributions of $P_c \rightarrow J/\psi$. The β 's values are different from different J^P of P_c . The J/ψ rapidity distributions are shown in Fig. 2 with the values of β . It can be seen that the rapidity distributions of J/ψ are different from three β values. We can determined the J^P of P_c from the rapidity distributions of J/ψ or proton because the rapidity distributions of proton are similar to J/ψ . However, it is not easy to distinguish the β from transverse

momentum distributions.

Moreover, for the vector meson production in electron-proton scattering, the cross section

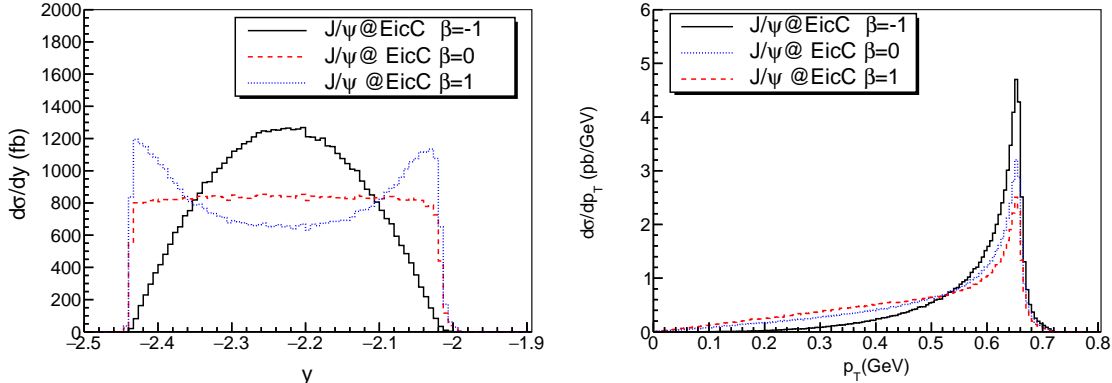


FIG. 2. (Color online) Rapidity distributions (left graph) and transverse momentum distributions (right graph) of J/ψ in $P_c(4312)$ exchange channel with the values of $\beta = -1$ (black solid curve) , $\beta = 0$ (red dashed curve) and $\beta = 1$ (blue dotted curve) at EicC.

of the Pomeron exchange t -channel is usually very large. Here we find it is much larger than that of P_c resonance channel. We give the distribution of final J/ψ produced from Pomeron and $P_c(4312)$ resonance at EicC in Fig.3. As can be seen, it is easy to distinguish two contributions by the rapidity distributions of J/ψ (or equally final proton). How to use this character to enhance the ratio of P_c to Pomeron by kinematic cut is detailed explored in a recent paper [52].

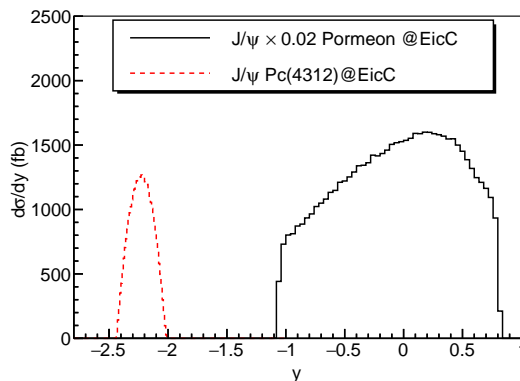


FIG. 3. (Color online) Rapidity distributions of J/ψ produced from Pomeron exchange channel (black solid curve) and $P_c(4312)$ ($J^P = (\frac{1}{2})^-$) resonance channel (red dashed curve) at EicC.

What's more, we give the rapidity distributions and transverse momentum distributions of J/ψ produced in $P_c(4312)$ resonance channel at EICs in Fig.4, where we assume the J^P of $P_c(4312)$ is $(\frac{1}{2})^-$. The same distributions of final proton are shown in Fig.5. The transverse momentum distributions is peaked at the range of $0.6 \sim 0.7$ GeV for different EICs, mainly due to the narrow widths of P_c states. The produced final particles at EicC are closer to the mid-rapidity than those at eRHIC.

Finally, the distributions of final leptons decaying from J/ψ are very important for the estimation of detector efficiency. We present the pseudo-rapidity distributions and transverse

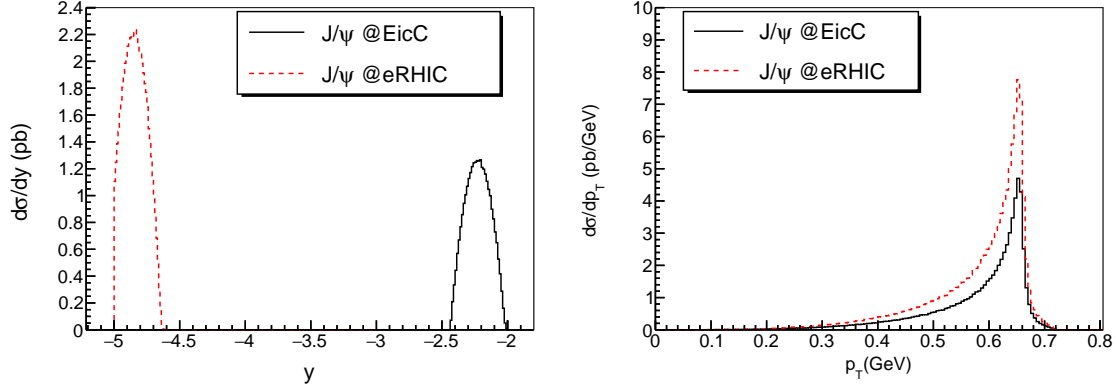


FIG. 4. (Color online) Rapidity distributions (left graph) and transverse momentum distributions (right graph) of J/ψ in $P_c(4312)$ ($J^P = (\frac{1}{2})^-$) resonance channel at EicC (black solid curve) and eRHIC (red dashed curve).

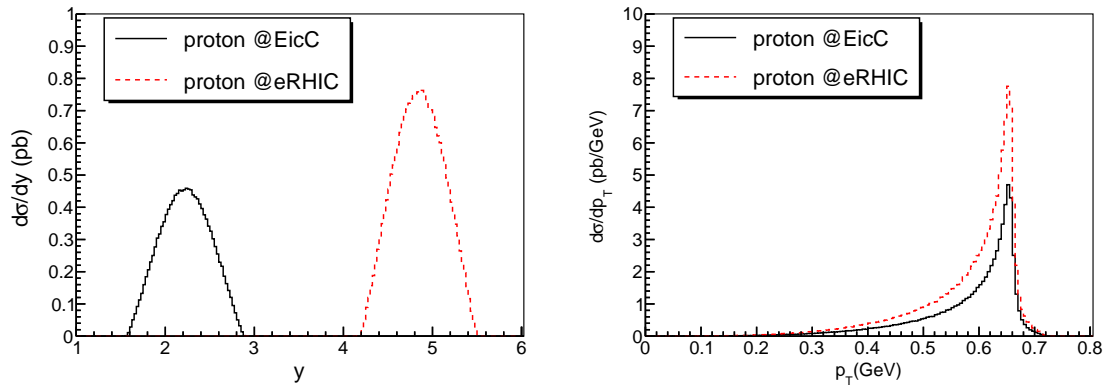


FIG. 5. (Color online) Rapidity distributions (left graph) and transverse momentum distributions (right graph) of proton in $P_c(4312)$ ($J^P = (\frac{1}{2})^-$) resonance channel at EicC (black solid curve) and eRHIC (red dashed curve).

momentum distributions of one of leptons decaying from J/ψ in $P_c(4312)$ resonance channel in Fig. 6. It can be seen that the daughter leptons from J/ψ decay at EicC are near middle pseudo-rapidity, which is easier to be detected.

These results in this section are useful for the proposed EICs including EicC and eRHIC. It can help us to check the models for the structure of the pentaquark states. We can use the rapidity distributions of J/ψ or proton to determined the spin and parity quantum number of P_c states.

IV. CONCLUSION

The study of P_c states in decays and reactions other than Λ_b decay plays a key role in our understanding of the nature of P_c states. In this paper we explore the electroproduction of pentaquark P_c in $ep \rightarrow epJ/\psi$ reaction for EicC and eRHIC in a detail. For this purpose, the eSTARlight package is adapted to include both s - and t -channel processes, considering their different kinematical conditions. The production rates are estimated, which seems to

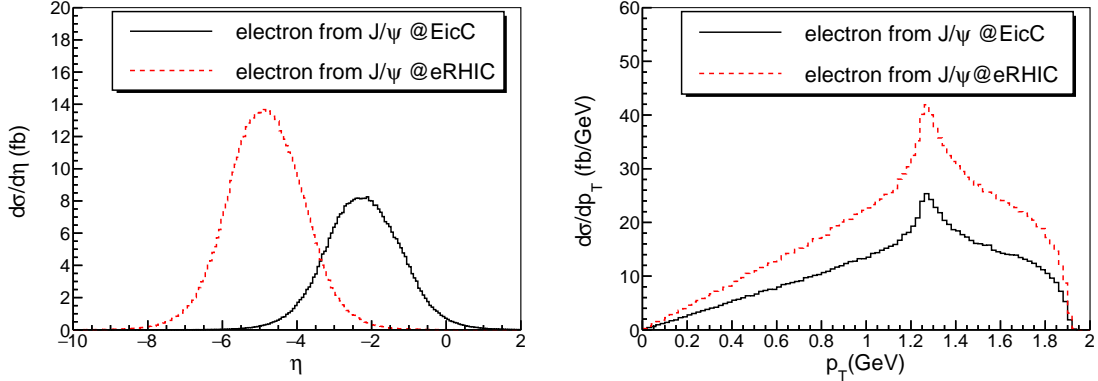


FIG. 6. (Color online) Pseudo-rapidity distributions (left graph) and Transverse momentum distributions (right graph) of one electron decaying from J/ψ in $P_c(4312)$ ($J^P = (\frac{1}{2})^-$) resonance channel for proposed EicC (black solid curve) and eRHIC (red dashed curve).

be large enough for detailed studies of these final states at EICs. The production cross sections depend on the internal structure of P_c , so electroproduction and photoproduction can test whether the P_c are real resonance or just peaks from triangle singularity. The different kinematic distributions of various contributions would be further reinforce this purpose, because the rapidity distributions of J/ψ and proton through pentaquark P_c decay and Pomeron exchange channel can distinguish two contributions clearly. This is confirmed by a recent study of how to enhance the signal of P_c by kinematic cut [52].

The rapidity distributions and transverse momentum distributions of final particles are compared here under various energy configuration at proposed EICs. It can conclude that the rapidity distributions of J/ψ or proton can be employed to determined the J^P of P_c states. This is important in our work. It can help us to determined the spin and parity of P_c states in EICs. Generally speaking, we find that the production cross sections increase slowly with the growing c.m. energies of EIC machine. At high-energy colliders like the proposed eRHIC, the final states are produced at far forward rapidities. For lower energy colliders like EicC, the systems are produced closer to midrapidity, within reach of central detectors.

Our study is a good start point to a further detailed simulation of P_c or even P_b electroproduction process, which will be helpful for the design of experimental method and detector system at EICs. As the EICs are expected to be in operation in near future and unavailable at present, alternative way at hand would be the ultra-peripheral lead-lead and pA collisions at STAR and ALICE [53]. The vector meson production in heavy ions ultra-peripheral collisions can be simulated by STARlight package [51] and the production of pentaquark can be included by a similar extension of kinematic condition in this paper.

ACKNOWLEDGMENT

The authors thank gratefully to the discussions with Dr. J. J. Xie, Dr. Z. Yang, Dr. X.Y.Wang and Dr. J. J. Wu. The work is supported by the National Natural Science Foundation of China (Grant Nos. 11975278, 11405222), and by the Key Research Program

- [1] H. X. Chen, W. Chen, X. Liu and S. L. Zhu, Phys. Rept. **639**, 1 (2016) [arXiv:1601.02092 [hep-ph]].
- [2] F. K. Guo, C. Hanhart, U. G. Meißner, Q. Wang, Q. Zhao and B. S. Zou, Rev. Mod. Phys. **90**, no. 1, 015004 (2018) [arXiv:1705.00141 [hep-ph]].
- [3] R. F. Lebed, R. E. Mitchell and E. S. Swanson, Prog. Part. Nucl. Phys. **93**, 143 (2017) [arXiv:1610.04528 [hep-ph]].
- [4] A. Esposito, A. Pilloni and A. D. Polosa, Phys. Rept. **668**, 1 (2017) [arXiv:1611.07920 [hep-ph]].
- [5] S. L. Olsen, T. Skwarnicki and D. Zieminska, Rev. Mod. Phys. **90**, no. 1, 015003 (2018) [arXiv:1708.04012 [hep-ph]].
- [6] Y. R. Liu, H. X. Chen, W. Chen, X. Liu and S. L. Zhu, Prog. Part. Nucl. Phys. **107**, 237 (2019) [arXiv:1903.11976 [hep-ph]].
- [7] N. Brambilla, S. Eidelman, C. Hanhart, A. Nefediev, C. P. Shen, C. E. Thomas, A. Vairo and C. Z. Yuan, arXiv:1907.07583 [hep-ex].
- [8] A. Ali, J. S. Lange and S. Stone, Prog. Part. Nucl. Phys. **97**, 123 (2017) [arXiv:1706.00610 [hep-ph]].
- [9] R. Aaij *et al.* [LHCb Collaboration], Phys. Rev. Lett. **115**, 072001 (2015) [arXiv:1507.03414 [hep-ex]].
- [10] R. Aaij *et al.* [LHCb Collaboration], Phys. Rev. Lett. **122**, no. 22, 222001 (2019) [arXiv:1904.03947 [hep-ex]].
- [11] V. M. Abazov *et al.* [D0 Collaboration], arXiv:1910.11767 [hep-ex].
- [12] A. Ali *et al.* [GlueX Collaboration], Phys. Rev. Lett. **123**, no. 7, 072001 (2019) [arXiv:1905.10811 [nucl-ex]].
- [13] J. J. Wu, R. Molina, E. Oset and B. S. Zou, Phys. Rev. Lett. **105**, 232001 (2010) [arXiv:1007.0573 [nucl-th]].
- [14] J. J. Wu, R. Molina, E. Oset and B. S. Zou, Phys. Rev. C **84**, 015202 (2011) [arXiv:1011.2399 [nucl-th]].
- [15] J. B. Cheng and Y. R. Liu, Phys. Rev. D **100**, no. 5, 054002 (2019) [arXiv:1905.08605 [hep-ph]].
- [16] A. Ali and A. Y. Parkhomenko, Phys. Lett. B **793**, 365 (2019) [arXiv:1904.00446 [hep-ph]].
- [17] A. Ali, I. Ahmed, M. J. Aslam, A. Y. Parkhomenko and A. Rehman, JHEP **1910**, 256 (2019) [arXiv:1907.06507 [hep-ph]].
- [18] M. I. Eides, V. Y. Petrov and M. V. Polyakov, arXiv:1904.11616 [hep-ph].
- [19] F. K. Guo, U. G. Meißner, W. Wang and Z. Yang, Phys. Rev. D **92**, no. 7, 071502 (2015) [arXiv:1507.04950 [hep-ph]].
- [20] X. H. Liu, Q. Wang and Q. Zhao, Phys. Lett. B **757**, 231 (2016) [arXiv:1507.05359 [hep-ph]].
- [21] X. H. Liu and M. Oka, Nucl. Phys. A **954**, 352 (2016) [arXiv:1602.07069 [hep-ph]].
- [22] F. K. Guo, U. G. Meißner, J. Nieves and Z. Yang, Eur. Phys. J. A **52**, no. 10, 318 (2016) [arXiv:1605.05113 [hep-ph]].
- [23] M. Bayar, F. Aceti, F. K. Guo and E. Oset, Phys. Rev. D **94**, no. 7, 074039 (2016) [arXiv:1609.04133 [hep-ph]].

- [24] X. H. Liu, G. Li, J. J. Xie and Q. Zhao, Phys. Rev. D **100**, no. 5, 054006 (2019) [arXiv:1906.07942 [hep-ph]].
- [25] F. K. Guo, X. H. Liu and S. Sakai, arXiv:1912.07030 [hep-ph].
- [26] Q. Wang, X. H. Liu and Q. Zhao, Phys. Rev. D **92**, 034022 (2015) [arXiv:1508.00339 [hep-ph]].
- [27] M. Karliner and J. L. Rosner, Phys. Lett. B **752**, 329 (2016) [arXiv:1508.01496 [hep-ph]].
- [28] V. Kubarovsky and M. B. Voloshin, Phys. Rev. D **92**, no. 3, 031502 (2015) [arXiv:1508.00888 [hep-ph]].
- [29] Y. Huang, J. J. Xie, J. He, X. Chen and H. F. Zhang, Chin. Phys. C **40**, no. 12, 124104 (2016) [arXiv:1604.05969 [nucl-th]].
- [30] A. N. Hiller Blin, C. Fernandez-Ramirez, A. Jackura, V. Mathieu, V. I. Mokeev, A. Pilloni and A. P. Szczepaniak, Phys. Rev. D **94**, no. 3, 034002 (2016) [arXiv:1606.08912 [hep-ph]].
- [31] J. J. Wu, T.-S. H. Lee and B. S. Zou, Phys. Rev. C **100**, no. 3, 035206 (2019) [arXiv:1906.05375 [nucl-th]].
- [32] X. Y. Wang, X. R. Chen and J. He, Phys. Rev. D **99**, no. 11, 114007 (2019) [arXiv:1904.11706 [hep-ph]].
- [33] Q. F. Lü, X. Y. Wang, J. J. Xie, X. R. Chen and Y. B. Dong, Phys. Rev. D **93**, no. 3, 034009 (2016) [arXiv:1510.06271 [hep-ph]].
- [34] X. Y. Wang, J. He, X. R. Chen, Q. Wang and X. Zhu, Phys. Lett. B **797**, 134862 (2019) [arXiv:1906.04044 [hep-ph]]. [35]
- [35] S. H. Kim, H. C. Kim and A. Hosaka, Phys. Lett. B **763**, 358 (2016) [arXiv:1605.02919 [hep-ph]].
- [36] M. Z. Liu, Y. W. Pan, F. Z. Peng, M. Sanchez Snchez, L. S. Geng, A. Hosaka and M. Pavon Valderrama, Phys. Rev. Lett. **122**, no. 24, 242001 (2019) [arXiv:1903.11560 [hep-ph]].
- [37] C. W. Xiao, J. Nieves and E. Oset, Phys. Rev. D **100**, no. 1, 014021 (2019) [arXiv:1904.01296 [hep-ph]].
- [38] M. L. Du, V. Baru, F. K. Guo, C. Hanhart, U. G. Meißner, J. A. Oller and Q. Wang, arXiv:1910.11846 [hep-ph].
- [39] J. J. Wu and B. S. Zou, Phys. Lett. B **709**, 70 (2012) [arXiv:1011.5743 [hep-ph]].
- [40] C. W. Xiao and E. Oset, Eur. Phys. J. A **49**, 139 (2013) [arXiv:1305.0786 [hep-ph]].
- [41] M. Karliner and J. L. Rosner, Phys. Rev. Lett. **115**, no. 12, 122001 (2015) doi:10.1103/PhysRevLett.115.122001 [arXiv:1506.06386 [hep-ph]].
- [42] X. Cao, F. K. Guo, Y. T. Liang, J. J. Wu, J. J. Xie, Y. P. Xie, Z. Yang and B. S. Zou, arXiv:1912.12054 [hep-ph].
- [43] X. Cao and J. p. Dai, Phys. Rev. D **100**, no. 5, 054033 (2019) [arXiv:1904.06015 [hep-ph]].
- [44] M. Lomnitz and S. Klein, Phys. Rev. C **99**, no. 1, 015203 (2019) [arXiv:1803.06420 [nucl-ex]].
- [45] S. R. Klein and Y. P. Xie, Phys. Rev. C **100**, no. 2, 024620 (2019) [arXiv:1903.02680 [nucl-th]].
- [46] Xu Cao, Lei Chang, Ningbo Chang, *et al.*, *Electron Ion Collider in China (in Chinese)*, Nuclear Techniques, 2020, 43(2): 020001.
- [47] X. Chen, PoS DIS **2018**, 170 (2018) [arXiv:1809.00448 [nucl-ex]].
- [48] V. Morozov, Presented at the EIC Users Group Meeting 2017, Trieste, Italy, (2017).
- [49] J. L. Abelleira Fernandez *et al.* [LHeC Study Group], J. Phys. G **39**, 075001 (2012) [arXiv:1206.2913 [physics.acc-ph]].
- [50] V. M. Budnev, I. F. Ginzburg, G. V. Meledin and V. G. Serbo, Phys. Rept. **15**, 181 (1975).
- [51] S. R. Klein, J. Nystrand, J. Seger, Y. Gorbunov and J. Butterworth, Comput. Phys. Commun. **212**, 258 (2017) [arXiv:1607.03838 [hep-ph]].
- [52] Z. Yang, X. Cao, Y. T. Liang and J. J. Wu, arXiv:2003.06774 [hep-ph].

[53] V. P. Goncalves and M. M. Jaime, arXiv:1911.10886 [hep-ph].